Quantification of Local Symmetry: Application for Texture Discrimination

Yoram Bonneh Daniel Reisfeld

Yehezkel Yeshurun

Department of Computer Science

Tel Aviv University, 69978 Tel Aviv, Israel.

Short title: Quantification of Local Symmetry

Communication address: Dr. Y. yeshurun, Dept. of CS, Tel Aviv University, Israel

Abstract

Symmetry is one of the most prominent cues in visual perception as well as in computer vision. We have recently presented the Generalized Symmetry Transform that receives as input an edge map, and outputs a symmetry map, where every point mark the intensity and orientation of the local generalized symmetry. In the context of Computer Vision, this map emphasizes points of high symmetry, which, in turn, are used to detect regions of interest for active vision systems. Many psychophysical experiments in texture discrimination use images that consist of various micro-patterns. Since the Generalize Symmetry Transform captures local spatial relations between image edges, we have used it to predict human performance in discrimination tasks. Applying the transform on micro-patterns of some well studied quantitative experiments of human texture discrimination, we show that symmetry, as characterized by our computational scheme, can account for most of them.

Keywords: Generalized Symmetry, Texture Discrimination, Regions of Interest.

1 Introduction

Symmetry is among the most prominent spatial relations perceived by humans. Natural and artificial objects often give rise to the human sensation of symmetry, and this sense of symmetry is so strong that the Gestalt school considered symmetry as a fundamental principle of perception. Looking around us, we get the immediate impression that practically every interesting visual area consists of some generalized form of symmetry.

We have recently presented a generalized symmetry transform and demonstrated its application to detection of interest points in natural images (Reisfeld, Wolfson, and Yeshurun ress) and for face recognition (Edelman, Reisfeld, and Y.Yeshurun 1992) and normalization (Reisfeld and Yeshurun 1992) tasks. Using this measure, we have suggested a computational model that takes as an input the intensity gradient at each image point, and generates activity maps of the generalized symmetry in different scales. Areas of different texture are thus characterized by different activity on one or more of these maps. The basis of our transform is the quantification of local spatial relations between image edges in a way that captures the amount of symmetry support at each point. For example, parallel centered intensity gradients strongly support a symmetry point between them while co-linear gradients do not. This quantification can be interpreted as an estimation of a local "Gestalt Glue". It computes points of interest, where attention might then be directed, e.g eyes of a person in a portrait or heads in a group of people (Reisfeld, Wolfson, and Yeshurun 1990). When applied more locally to images, it detects sharp corners as interest points by assigning high "symmetry" value. Applied to texture micro-patterns, it quantifies every micro-pattern, and thus can be used as the basis for discrimination. In this paper, we present the results of applying our measure to some well studied quantitative results in human psychophysics, and show that our simple model yields rather good fit to human performance.

2 Generalized Symmetry

In the usual mathematical notion, an object is regarded symmetric if it is invariant to the application of certain transformations, called symmetry operations. A typical symmetry operation is the well known reflectional (mirror) symmetry. In order to use these symmetry operations it is necessary to know the shape of an object before we can estimate whether it is symmetric or not. However, we wish to quantify symmetry without any prior knowledge of objects, especially if the symmetry measure is used to detect regions of interest.

Our symmetry transform does not require the knowledge of the object's shape. It performs local operations on the edges of the image. Moreover, it assigns a continuous symmetry measure to each point in the image, rather than a binary symmetry label.

We first define a symmetry measure for each point. Let $p_k = (x_k, y_k)$ be any point $(k = 1, \ldots, K)$, and denote by $\nabla p_k = \left(\frac{\partial}{\partial_x} p_k, \frac{\partial}{\partial_y} p_k\right)$ the gradient of the intensity at point p_k. We assume that a vector $v_k = (r_k, \theta_k)$ is associated with each p_k such that $r_k = \log(1 + \|\nabla p_k\|)$ and $\theta_k = \arctan\left(\frac{\partial}{\partial_y} p_k / \frac{\partial}{\partial_x} p_k\right)$. For each two points p_i and p_j, we denote by l the line passing through them, and by α_{ij} the angle counterclockwise between l and the horizon. We define the set $\Gamma(p)$, a distance weight function $D_\sigma(i,j)$, and a phase weight function $P(i,j)$ as

$$\begin{aligned}
\Gamma(p) &= \left\{(i,j) \,\middle|\, \frac{p_i + p_j}{2} = p\right\} \\
D_\sigma(i,j) &= G_\sigma(\|p_i - p_j\|) \\
P(i,j) &= (1 - \cos(\theta_i + \theta_j - 2\alpha_{ij}))(1 - \cos(\theta_i - \theta_j))
\end{aligned}$$

where $G_\sigma(t) = \frac{1}{\sqrt{2\pi}\sigma} \exp -\frac{t^2}{2\sigma^2}$ is the Gaussian, σ of D_σ corresponds to scale or a locality channel.

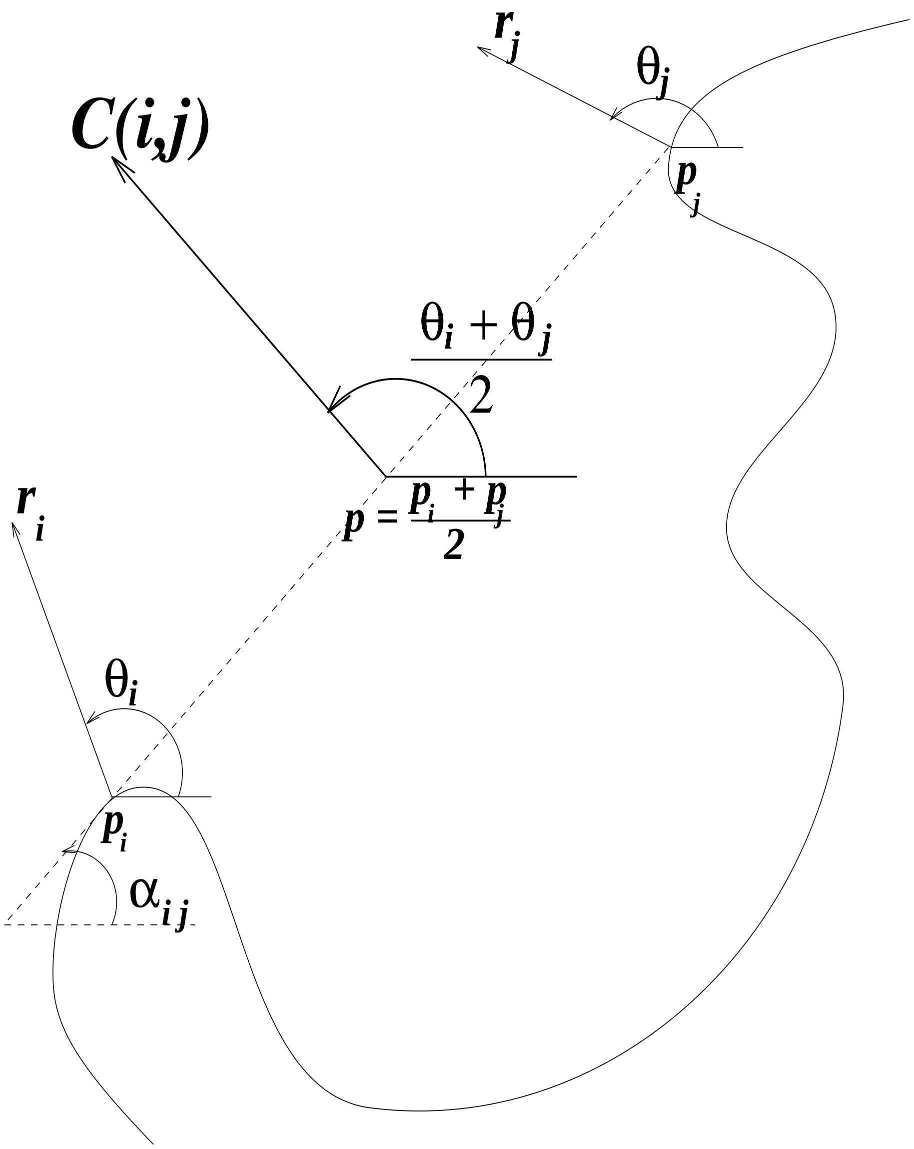

Figure 1: The contribution to symmetry of the gradients at p_i and p_j.

We define the contribution of the points p_i and p_j as

$$C(i,j) = D_\sigma(i,j)P(i,j)r_ir_j$$

This measure can be easily normalized, and reflects the fact that each of its components modulates the other ones. The *symmetry magnitude* or *isotropic symmetry* $M_\sigma(p)$ of each point p is defined as

$$M_\sigma(p) \quad = \sum_{(i,j)\in\Gamma(p)} C(i,j)$$

which averages the symmetry value over all orientations. We define the direction of the contribution of p_i and p_j as

$$\varphi(i,j) = \frac{\theta_i + \theta_j}{2}$$

The *symmetry direction* is defined as $\phi(p) = \varphi(i,j)$ such that $C(i,j)$ is maximal for $(i,j) \in \Gamma(p)$. Thus, the symmetry of the point p is defined as

$$S_\sigma(p) = (M_\sigma(p), \phi(p))$$

The demand that the symmetry transform be local is reflected by the Gaussian distance weight function, $D_\sigma(i,j)$. Different values for σ imply different scales, thus enabling convenient implementation of multi-resolution schemes. Note that the Gaussian defined above has circular isotherms, i.e. it has no preferred orientation. However, one can also define Gaussians with elliptic isotherms. This is useful when the transform is applied as a feature detector of elliptic regions such as eyes in human faces (Reisfeld and Yeshurun 1992). In the experimental results presented in this paper we have used only circular Gaussians.

The phase weight function, $P(i,j)$ is composed of two terms. The first term, $1 - \cos(\theta_i + \theta_j - 2\alpha_{ij})$, allows to achieve maximum symmetry when $(\theta_i - \alpha_{ij}) +$

$(\theta_j - \alpha_{ij}) = \pi$ i.e. when the gradients at p_i and p_j are oriented in the same direction towards each other. This is consistent with the intuitive notion of symmetry. This expression decreases continuously as the situation deviates from the ideal one. Notice that the same measure is achieved for various object reflectance and lighting situation, which are discussed in (Reisfeld et al. 1994).

The second term of $P(i,j)$, $1 - \cos(\theta_i - \theta_j)$, is introduced since the first term attains its maximum whenever $(\theta_i - \alpha_{ij}) + (\theta_j - \alpha_{ij}) = \pi$. This includes the case $\theta_i - \alpha_{ij} = \theta_j - \alpha_{ij} = \pi/2$, which occurs on a straight edge, which we do not regard as interesting. The current expression compensates for this situation.

The term $r_i r_j$ is high when there is a strong correlation between two large gradients. We use gradients rather than intensities since we are mainly interested in edges that relates to object borders. For instance, a uniform intensity wall is highly symmetric but probably not very interesting. In natural scenes we prefer to use the logarithm of magnitude instead of the magnitude itself, since it reduces the differences between high gradients, and therefore the correlation measure is less sensitive to very strong edges.

Sometimes it is necessary to detect points that are highly symmetric in multiple distinct orientations rather then in a principle one. We define such a symmetry as *radial symmetry* – $RS(p)$ and its value can be evaluated using the formula:

$$RS_\sigma(p) \quad = \sum_{(i,j)\in\Gamma(p)} C(i,j) \quad \sin^2(\varphi(i,j) - \phi(p))$$

This expression emphasizes contribution in the directions which are perpendicular to the main symmetry direction, and attains its maximum in a point that is surrounded by edges. Notice that due to the continuous nature of the operator, the radial symmetry is not sensitive to gaps in the contour that surrounds the point p, and does not require this contour to be uninterrupted.

The above definition is highly sensitive to the direction of contrast which is significant in evaluating symmetry of objects. Sometimes however, it is unimportant as in the case of texture micro-patterns or line drawings. A line, for example, should be treated as a single edge and not as a thin object. We define a variant of the symmetry transform by modifying the phase weight function so that edge orientation is used and direction of contrast ignored. Let $u_k = (r_k, \theta_k)$ be the edge at p_k such that r_k is the edge magnitude and $\theta_k \in [0, \pi]$ is the edge orientation. The texture variant of the phase weight function is given by

$$P'(i,j) \quad = \quad G_{\sigma_0}\left(\theta_i - \alpha_{ij} - \pi/2\right) G_{\sigma_0}\left(\theta_j - \alpha_{ij} - \pi/2\right)$$

Where G_σ is the Gaussian function as in the previous definition and the phase tuning σ_0 is fixed. When the edge orientations are co-linear there is no support for symmetry. The strongest support is when the two edge orientations are both orthogonal to the virtual line connecting the points, i.e. parallel centered. This is captured by a product of two Gaussian tuning functions which makes the phase function monotonic between these two extreme cases. The effect of this definition is similar to the one defined earlier when ignoring the direction of contrast. We use it in all the applications of the symmetry transform to textures.

In figure 3 we demonstrate the symmetry map produced by the transform on a (almost) natural image. As we show in (Reisfeld et al., In press), the symmetry transform generalizes most of the existing methods for detection of regions of interest in computer vision (e.g high curvature, density of edges, junctions). The peaks of intensity in the symmetry map are used to index regions of interest, and in figure 3 the highest peaks of the intensity map are the facial features. In figure 2 we present the symmetry map (texture variant) of various texture micro-patters, to demonstrate the motivation behind our approach, and to show that different micro-patterns are differently quantified by the transform. In the following we define in details the specific measure used for discrimination.

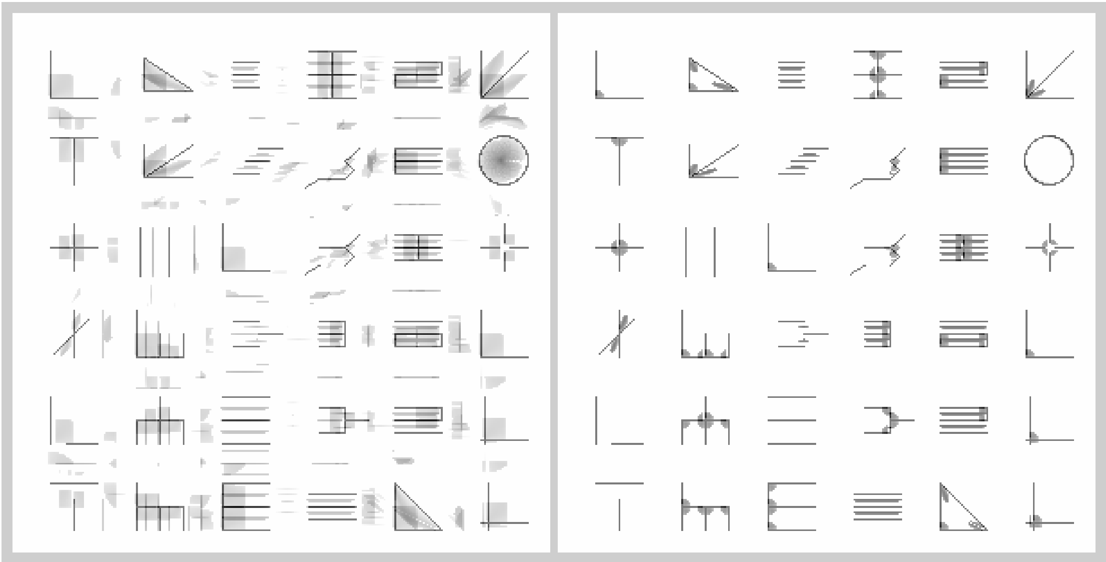

Figure 2: Some of the patterns used in the psychophysical experiments superimposed on their symmetry response. Right - the local channel ($\sigma = 2$), Left - a wide channel ($\sigma = 4$). The logarithm of the response of the radial symmetry is shown as gray level intensity

Figure 3: Detection of interest points using the generalized symmetry transform. (left to right) Original image; its edges; isotropic symmetry.

3 Models of Texture Discrimination and Segmentation

Humans are able to discriminate between surfaces sharing the same average color and brightness but differ in small scale luminance variations generally called texture. This ability is vital to segmentation since natural objects are often heterogeneous and their boundary cannot always be found by simple edge detectors. The classical work of Julesz claimed that texture discrimination could be explained in terms of global second order statistic differences between points in the image (Julesz 1975). Later work attributed the discrimination to first-order differences in features such as orientation, size and brightness of local texture elements. (Julesz 1981; Julesz 1986; Beck 1966; Beck 1983). The Texton theory (Julesz 1981) specified these elements as Textons, that are elongated blobs with specific color, orientation and size, line ends (terminators) and line crossings. Some theories (Marr 1982; Beck, Prazdny, and Rosenfield 1983) claim that a hierarchical grouping process links the basic features according to Gestalt rules (e.g. proximity, similarity and good continuation) and

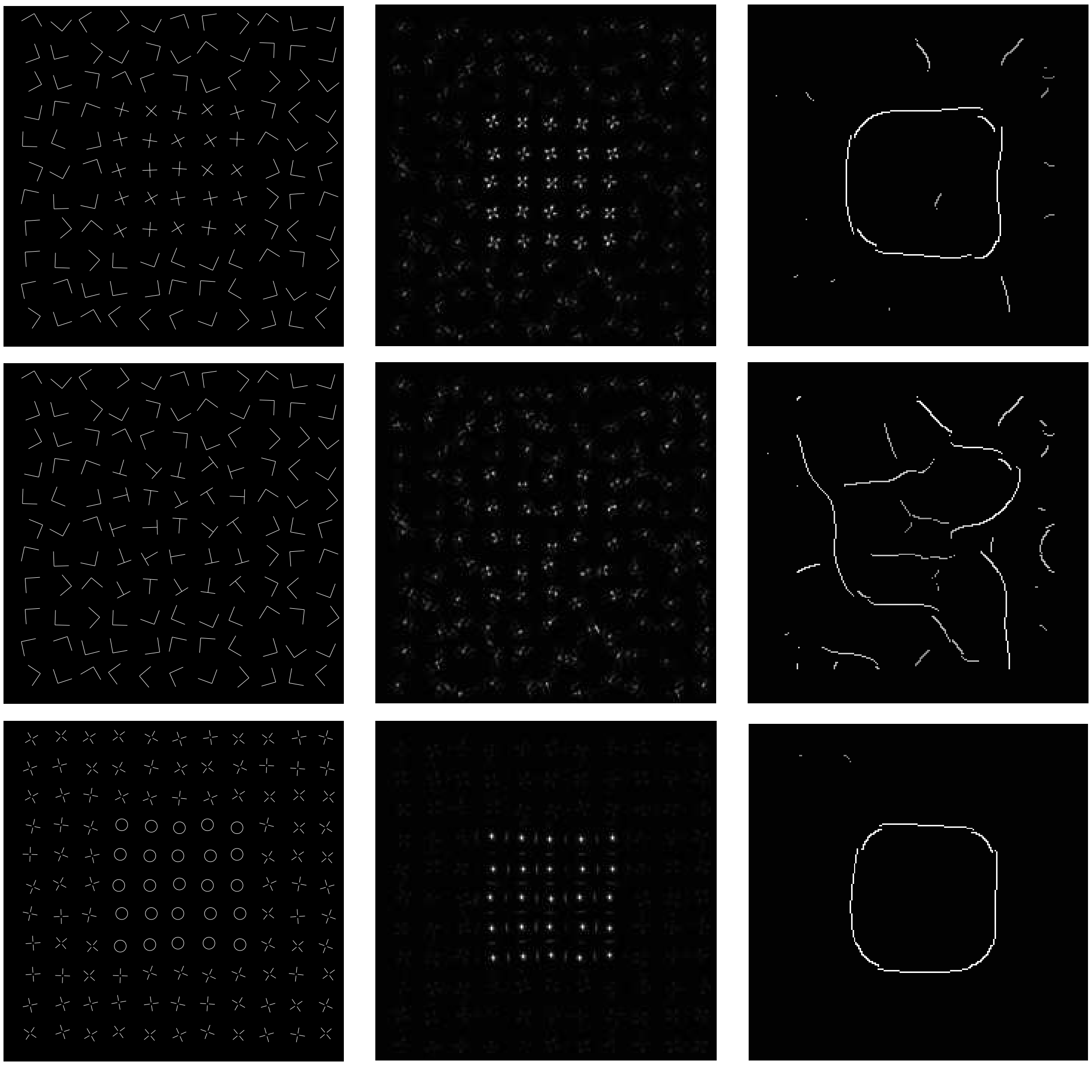

Figure 4: Artificial texture discrimination by the model. Left column - the textures, middle - local symmetry maps, right - computed boundaries.

texture boundaries are extracted from differences in these higher order elements. All these theories were based on a qualitative distinction between effortless *preattentive* texture discrimination and the more time consuming *attentive* discrimination.

Recent psychophysical experiments questioned the preattentive-attentive dichotomy and found graded discriminability in textures composed from randomly rotated patterns (similar to Figure 4) (Gurnsey and Browse 1987). Similar results were obtained in detection tasks (Krose 1987). They provide us with a database of discriminability measures for a set of randomly rotated artificial pattern pairs. These observations raised the need for a computational model that discriminates between textures in a continuous manner and can be quantitatively compared with human performance. Such models (Fogel and Sagi 1989; Malik and Perona 1990) are based on linear filters followed by a non-linear stage that produces activity maps where texture boundaries becomes activity gradient. Discrimination is then achieved by combining the gradients in the different maps followed by a decision stage that corresponds to subject's decision whether boundary exists or not. The effect of figure-ground asymmetry in discriminability is attributed to this decision stage (Rubenstein and Sagi 1990).

Other recent studies of computer vision (Porat and Zeevi 1989; Jain and Farrokhnia 1991; Bovik 1991; Dunn, Higgins, and Wakely 1994) and human texture discrimination are concerned with segmentation based on orientation and spatial frequency filters rather than with a direct quantification of micro-patterns spatial configuration. Nothdurft (Nothdurft 1991) demonstrated texture segmentation that arises from orientation differences rather than from the orientation features themselves. Landy and Bergen (Landy and Bergen 1991) studied orientation and scale difference and developed a full scale quantitative model based on linear filters in different orientations scales and energy summation. Their model matches orientation discrimination data but is not tested on micro-pattern textures. Hallet (Hallett 1992) developed mesh-derived textures and studied the effect of orientation and spatial disorder. His results show that orientation and position jitter of textural elements are often exchangeable, a fact that contradicts the common belief that de-emphasize the role of elements position (Julesz 1984).

4 Discrimination of Texture Micro-patterns by Generalized Symmetry

Almost all psychophysical studies of texture discrimination use artificial textures of various types and test their discriminability. The most popular paradigm uses split fields of randomly rotated micro-patterns. Figure 4 demonstrates the model's operation on such artificial textures. The top and middle rows demonstrate textures composed of X-L and L-T patterns. These textures are widely studied (Julesz 1984; Gurnsey and Browse 1987; Krose 1987; Fogel and Sagi 1989; Malik and Perona 1990; Bergen and Adelson 1988) since the X-L texture is easily discriminated while the L-T requires more time and attention. This was measured (among other pattern pairs) by Gurnsey and Browse (Gurnsey and Browse 1987) and in detection tasks that yield similar results by Krose (Krose 1987). The current explanations include the Texton theory (Julesz 1981) that attributes the X-L discrimination to a crossing texton, the size-tuning principle (Bergen and Adelson 1988) that attributes discrimination to difference in size, and models that define filter-based mechanisms producing the desired results (Fogel and Sagi 1989; Malik and Perona 1990).

These well known examples are shown in figure 4 along with their corresponding symmetry maps, in order to clarify the intuition behind our approach. The response for the X pattern consists of four components, the T of two and the L consists only of a single component. If discriminability is attributed to difference in the total amount of symmetry, then X-L should be discriminated much easier than the L-T. In order to make explicit use of the differences in the symmetry map, we used a simple low frequency edge detector that is applied to the symmetry map, to extract the texture boundaries. We emphasize that this stage was carried out as a demonstration only, since we do not present a complete texture segmentation algorithm, but rather a micro-pattern discrimination measure.

The boundary of the X-L texture is clearly visible (top right) while the boundary of the L-T texture is not clear although some fragments of it can be noticed.

The bottom row of Figure 4 demonstrates the discrimination of similar textures composed of X-O patterns studied by (Krose 1987). The computation is identical to that used for the other textures except for a wider symmetry channel ($\sigma = 4$, instead of $\sigma = 2$ used for the upper two rows). The model succeeds in computing explicit boundaries for this highly discriminable textures as displayed in bottom right. It is important to note that the discrimination of these artificial textures is a simple task and can be done in many different ways. The key point is not to segment these textures, but to match human performance in texture discrimination. Thus, we are looking for a measure that incorporates the response of all the symmetry channels, and can be compared to human performance.

4.1 The Discriminability Measure

In order to compare our model to human performance, we define a discriminability measure between micro-pattern pairs. The symmetry measure for a micro-pattern m, which is a small binary image, is the log of the sum of a symmetry measure ,SM (which can be the isotropic symmetry, the radial symmetry etc.), of all its points:

$$R_\sigma(m) = \log \left(\sum_{p \in m} SM_\sigma(p) \right)$$

The *discriminability measure* between two micro-patterns $m1$ and $m2$ in a channel determined by σ is defined as

$$DM_\sigma(m,n) = \|R_\sigma(m) - R_\sigma(n)\|$$

The (total) discriminability is

$$DM(m,n) = \max_\sigma D_\sigma(m,n)$$

which is the maximal response over all channels. This is a natural extension to models of brightness perception (e.g (Land and McCann 1971)), since the luminance and the symmetry edges might be computed in a similar way. In the following, we have actually used the radial symmetry (RS_σ) as the specific symmetry measure, and two channels.

4.2 Results

We applied this computation to the patterns studied by Gurnsey & Browse (Gurnsey and Browse 1987) and Krose (Krose 1987) using 30×30 pixel patterns, 2 channels with $\sigma = 7$ and $\sigma = 40$ (in pixels) and $\sigma_0 = 0.125$ for the phase function (see definition of the transform). Results appear in Figure 5. The black bars represent human discrimination power, where higher value stands for easier discrimination. The gray bars represent the model's discriminability values after linear normalization. The pair numbers follow the data from (Gurnsey and Browse 1987) and can be used for reference. The computed correlation of the bottom table which corresponds to the experiments of Gurnsey & Browse (Gurnsey and Browse 1987) is $\rho = 0.93$. We also tested our model with data from Krose (Krose 1987) which appear in the top charts. The received correlation is $\rho = 0.86$ and $\rho = 0.98$ for the 2 experiments. These values are better than those reported previously (Fogel and Sagi 1989; Krose 1987).

4.3 Figure-ground asymmetry

The asymmetry of figure-ground in texture discrimination is found in (Gurnsey and Browse 1987; Willliams and Julesz 1992) and in similar detection tasks in (Triesman 1988) and is modeled in (Rubenstein and Sagi 1990). For example, it is easier to detect a square of L patterns embedded in surrounding X patterns than vise versa. In testing our model, we have used so far the reported average discriminability as done by others (Malik and Perona 1990; Fogel and Sagi 1989). A more careful investigation of the model's computed symmetry values shows that patterns of higher symmetry are a preferred background. This is formulated as a modification to the discriminability measure defined earlier:

$$DM_\sigma(g,t) = |SM_\sigma(g) - SM_\sigma(t)| + k * (SM_\sigma(g) - SM_\sigma(t))$$

where g, t are the ground and target patterns respectively and $k < 1$ is a weight constant. The total discriminability is taken to be the maximal response over all channels as in the symmetric model.

We applied the modified model to the data from (Gurnsey and Browse 1987) using $k = 0.3$ and all other parameters as in the symmetric case. Results appear in Figure 6. The graph is similar to the previous symmetric case except that for each pattern pair there are two pairs of bars. The left/right pair correspond to the left/right pattern being the target. Again, the black bars represent human discrimination power and the gray bars represent the model's discriminability values. The computed correlation is $\rho = 0.84$. It is slightly smaller than reported previously (Rubenstein and Sagi 1990). The value of k is not that critical and similar correlations are obtained for k between 0.1 and 0.4.

5 Discussion

We have described a method for quantification of local generalized symmetry in images, that operates on edge images and produces a symmetry map. We have demonstrated its use for detection of region of interest, which is mainly relevant to computer vision, and presented a simple model, based on generalized symmetry, that shows good correlation with psychophysical data of texture discrimination tasks.

Since there are few factors involved in the computation, we tested the significance of each to the final result. First we consider locality. Since the symmetry transform is local, as expressed in its distance weight function, one may suspect that locality *per se* is sufficient, suggesting that discrimination may be merely based on evaluating the size of the micro-patterns and comparing it for both textures (Bergen and Adelson 1988). Bergen & Adelson (Bergen and Adelson 1988) demonstrated this principle using the rectified Laplacian of Gaussian. We have tested a variant of the symmetry model, which stress this locality idea, by neglecting the phase component. This decreases the correlation to the psychophysical data of Gurnsey & Browse to 0.73 instead of 0.93 that the full model achieves. This degradation is mainly due to micro-patterns with identical second order statistics like pair 3.1 in Figure 5. It is clear, however, that the main factor in the discrimination of the textures we have tested is indeed size (as already noted by Gurnsey & Browse). Our model captures size with its local Gaussian weighting function and its non-linear operation (the conjunction of pairs of edge points). There might be alternative ways to capture it.

Next we consider the radial symmetry and the need for actual symmetry maps. Using Isotropic symmetry instead, decreases correlation to 0.85 for the Gurnsey & Browse data and 0.82, 0.98 for the data from Krose. Again, there is a specific problem with the patterns with identical second order statistics, so the total correlation is somewhat misleading. There is however, an advantage in using the isotropic sym-

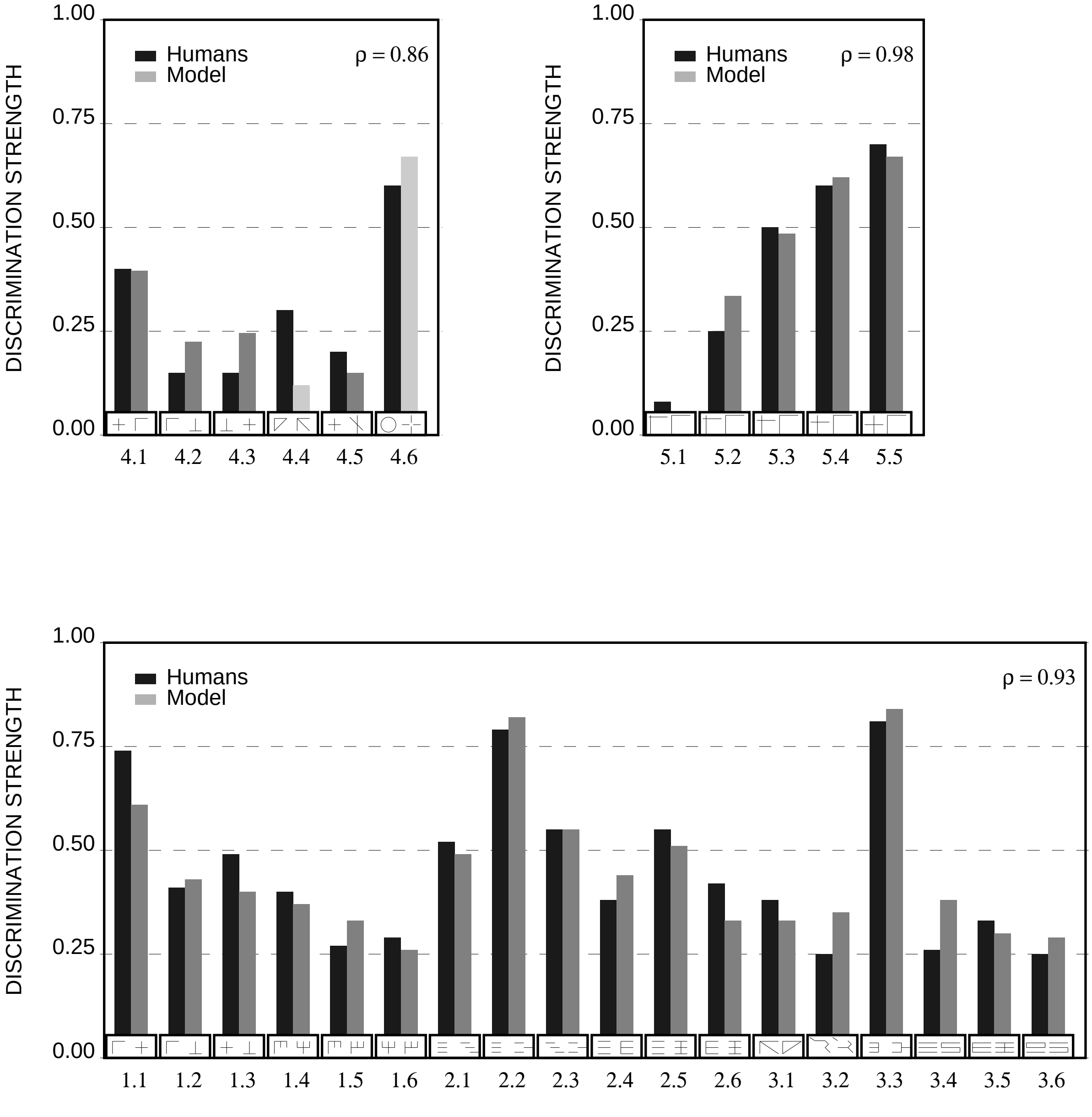

Figure 5: Model results Vs. human performance measured in psychophysical experiments. For each micro-pattern pair, human performance is denoted by the probability for correct detection in the experiments and the model's value denotes the discrimination measure. Human performance in bottom table is due to Gurnsey and Browse , upper tables are due to Krose. Numbers below the pairs are the labels of the patterns in the original papers

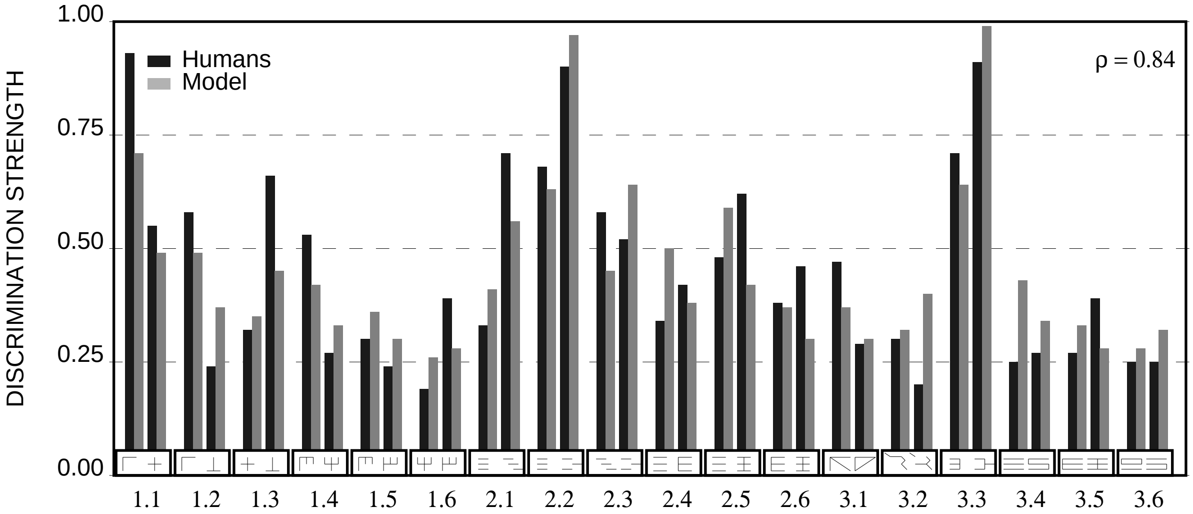

Figure 6: Model results Vs. human asymmetric performance measured in the psychophysical experiments of Gurnsey and Browse. For each micro-pattern pair, there are two pairs of bars where the left/right pair corresponds to the left/right pattern being the target respectively. Human performance is denoted by the probability for correct detection in the experiments and the model's value denotes the discrimination measure.

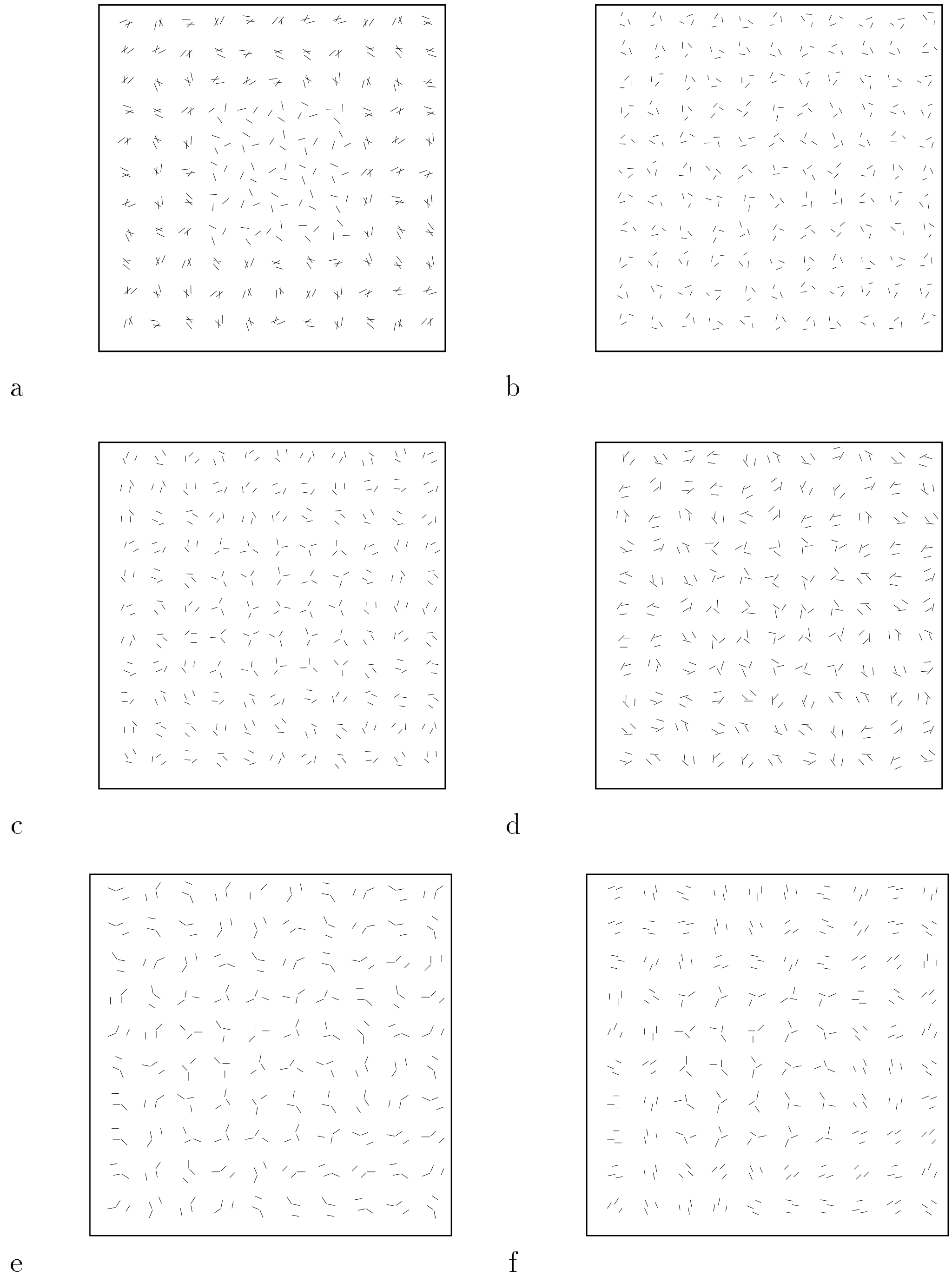

Figure 7: Randomly generated 3 line pattern textures. a - strong discriminability predicted, probably due to the locality Gaussian. b - very weak discriminability predicted. c,d,e,f - textures with similar second order statistics, predicted to have medium level discriminability.

metry. In this case the model is reduced to a simpler quantification of local spatial relations.

The figure-ground asymmetry effect is addressed in our work by modifying the symmetry measure to reflect the ratio between the background and foreground symmetry measures. The relative success of this formulation can be interpreted as another effect of size tuning: it is easier to detect large patterns among a background of small ones than the other way around. However, further inspection of figure-ground asymmetry evidence (Triesman 1988; Willliams and Julesz 1992) does not fully support this idea. Instead, it seems that the general principle behind all cases is that the more symmetric pattern is a "better" background. For example, a circle is a more symmetrical pattern than ellipse, so it is easier to detect ellipses among circles as background than vice versa. A full quantified explanation of the perceptual asymmetries in discrimination and detection tasks is left for future work.

Next we would like to point out that the set of patterns used in texture psychophysics is somewhat biased. Most of it was constructed in order to demonstrate a specific principle or theory. Therefore, it is possible that these patterns, that are traditionally used as test data, are not sufficient for the purpose of assessing new algorithms and theories. We have, therefore, constructed a data base of 10^4 micro-patterns by generating patterns composed of three line segments whose position is selected at random (see Figure 7). This might be the first step towards constructing a large data base of artificial textures that could be used for evaluating computational models for texture discrimination.

We hypothesize that patterns that differ in their generalized symmetry are easily discriminated by humans and vice versa, and suggest to use textures from this data base in order to verify it. In order to exclude other factors, like differences in the second order statistics, patterns with similar second order statistics were selected by an automatic exhaustive search from this database of 10^4 randomly generated patterns.

This was done by an explicit computation and comparison of the dot distance distribution (neglecting the orientation since the patterns are randomly rotated). Figure 7 demonstrates some of these textures tested by the model. (a) consists of textures predicted to have high discriminability. This may be attributed to the different size of the patterns captured by the locality Gaussian. (b) consists of a texture predicted to be almost indiscriminable (having tiny discriminability measure). (c),(d),(e),(f) consist of textures with similar second order statistics predicted to have some discriminability. We suggest that a systematic and quantitative analysis of randomly generated patterns might prove useful for further evaluation of models and algorithms for texture discrimination.

Our model should be compared with previous models (Fogel and Sagi 1989; Rubenstein and Sagi 1990; Malik and Perona 1990; Landy and Bergen 1991; Krose 1987; Bergen and Adelson 1988; Buf and Heitger 1993) in terms of fitting the psychophysical data, computational efficiency and biological plausibility. The model fits the average figure-ground discriminability measured in the Gurnsey & Browse experiments (Gurnsey and Browse 1987) better than any other model (not all provide quantitative match). Computationally, our model is somewhat different from the filter-based models mentioned previously (Fogel and Sagi 1989; Malik and Perona 1990; Landy and Bergen 1991). These models are defined in the level of neural mechanism inspired by cells in the visual cortex. Their discrimination is based on the responses of filters whose size is not smaller than a micro-pattern such that the main computation is done by the filters. When larger patterns are used, larger receptive fields are assumed, ignoring the computation carried out by the cells with the smaller receptive fields. Indeed, our approach is based on a simple and intuitive quantification of the generalized symmetry, and does not explicitly embark from current cortical models. However, if we examine the biological plausibility of our model, it turns out that it perfectly fits a view of the primary visual cortex as a network that analyzes local spatial configurations of edges. (Zucker, Dobbins, and Iverson 1989). According to this model, V1 can be viewed in a level that is higher than a set of filters, namely, it is a network where every cell responds to a given range of edge orientation and size, but there are lateral connections between cells that give rise to the notion of curvature, for example. The same network that estimates curvature, can quantify every image area according to our algorithm, thus enabling a direct segregation of texture. Another alternative is the computation of symmetry maps as defined by the model. Each symmetry cell in such a map integrates pairs of V1 simple cells in the proper orientations using Sigma-Pi connections (sum of the product of each pair). There is currently no evidence for such maps although some similarity can be found in V2 cells that respond to illusory contours, probably by integrating orientation selective cells in V1 (Heitger, Rosenthaler, Heydt, Peterhans, and Kubler 1992).

While offering a good fit for psychophysical data, symmetry quantification should be viewed as part of a larger process. The generalized symmetry model may be a part of an hierarchical texture processing system in which the lowest level might compute simple Texton differences (orientation, size, color, contrast) in low resolution; the next level quantifies local spatial relations based on local generalized symmetry; and the highest level may perform grouping processes as suggested by Beck (Beck 1983).

References

Beck, J. (1966). Effect of orientation and of shape similarity on grouping. *Percept. Psychophys. 1*, 300–302.

Beck, J. (1983). Textural segmentation, Second order statistics, and Textural elements. *Biol. Cybern. 48*, 125–130.

Beck, J., K. Prazdny, and A. Rosenfield (1983). A theory of texture segmentation.

In J. Beck and A. Rosenfield (Eds.), *Human and machine vision.* Academic Press Inc.

Bergen, J. R. and E. H. Adelson (1988). Early vision and texture perception. *Nature 333*, 363–364.

Bovik, A. C. (1991). Analysis of Multichannel narrow band filters for Image Texture Segmentation. *IEEE Trans. Signal Proc. 39*, 2025–2043.

Buf, J. D. and F. Heitger (1993). A Neural Network for detecting Symmetry Orders. In *Proc. 7th Int. Conf. on Image Analysis, Bari, Italy.*

Dunn, D., W. E. Higgins, and J. Wakely (1994). Texture Segmentation Using 2D Gabor Elementary Functions. *IEEE Trans. Pattern Anal. Machine Intell. PAMI-16*(2), 130–149.

Edelman, S., D. Reisfeld, and Y.Yeshurun (1992, May). Learning to recognize faces from examples. In *Second European Conference on Computer Vision*, S. Margherita, Ligure - Italy.

Fogel, I. and D. Sagi (1989). Gabor filters as texture descriminator. *Biological Cybernetics 61*, 103–113.

Gurnsey, R. and A. Browse (1987). Micropattern properties and presentation conditions influencing visual texture discrimination. *Percept. Psychophys. 41*(3), 239–252.

Hallett, P. E. (1992). Segregation of mesh-derived textures evaluated by resistance to added disorder. *Vision Res. 32*(10), 1899–1911.

Heitger, F., L. Rosenthaler, R. V. D. Heydt, E. Peterhans, and O. Kubler (1992). Simulation of neural contour mechanisms: from simple to end-stopped cells. *Vision Res. 32*(5), 963–981.

Jain, A. K. and F. Farrokhnia (1991). Unsupervised Texture Segmentation using Gabor Filters. *Pattern Recognition 23*, 1167–1185.

Julesz, B. (1975). Experiments in the visual perception of texture. *Scientific American 232*, 34–43.

Julesz, B. (1981). Textons, the elements of texture perception and their interactions. *Nature 290*, 91–97.

Julesz, B. (1984). Toaward an axiomatic theory of preattentive vision. In C. W. Edelman GM, Gall WE (Ed.), *Dynamic aspects of neocortical function*, pp. 585–612. Neurosciences Research Foundation.

Julesz, B. (1986). Texton gradients: The texton theory revisited. *Biological Cybernetics 54*, 245–251.

Krose, B. J. (1987). Local structure analyzers as determinants of preattentive texture discrimination. *Biol. Cybern. 55*, 289–298.

Land, E. and J. J. McCann (1971). Lightness and retinex theory. *J. Opt. Soc. Am. 61*(1), 1–11.

Landy, M. S. and J. R. Bergen (1991). Texture segregation and orientation gradient. *Vision Res. 31*, 679–691.

Malik, J. and P. Perona (1990). Preattentive texture discrimination with early vision mechanisms. *J. Opt. Soc. Am. 7*(5), 923–932.

Marr, D. (1982). *Vision*. Freeman.

Nothdurft, H. (1991). Texture segmentation and pop-out from orientation contrast. *Vision Res. 31*(6), 1073–1078.

Porat, M. and Y. Zeevi (1989). Localized Texture Processing in Vision: Analysis and Synthesis in the Gaborian Space. *IEEE Trans. Biomedical Eng. 36*, 115–129.

Reisfeld, D., H. Wolfson, and Y. Yeshurun (1990, December). Detection of interest point using symmmetry. In *Third International Conference on Computer Vision*, Osaka, Japan, pp. 62–65.

Reisfeld, D., H. Wolfson, and Y. Yeshurun (In Press). Context Free Attentional Operators: the Generalized Symmetry Transform. *Int. J. of Computer Vision*.

Reisfeld, D. and Y. Yeshurun (1992, September). Robust detection of facial features by generalized symmetry. In *Proceedings of the 11th International Conference on Pattern Recognition*, The Hague, Netherlands.

Rubenstein, B. S. and D. Sagi (1990). Spatial variability as a limiting factor in texture discrimination tasks: Implecations for performance asymmetries. *J. Opt. Soc. Am. 7*, 1632–1643.

Triesman, A. (1988). Feature analysis in early vision: evidence from search asymmetries. *Psychological Review 95*, 15–48.

Willliams, D. and B. Julesz (1992). Filters versus textons in human and machine texture discrimination. In H. Wechsler (Ed.), *Neural networks for perception*, Volume 1, pp. 145–175. Academic Press Inc.

Zucker, S. W., A. Dobbins, and L. Iverson (1989). Two stages of curve detection suggest two styles of visual computation. *Neural Computation 1*, 68–81.